Compact Triple-Band Monopole Antenna with ACS-Fed for IoT Devices on WLAN/WiMAX/5G/V2X Networks

Yusnita Rahayu[1,*], Dimas Rama Adji Pangestu[1], and Chia Hao Ku[2]
[1] Department of Electrical Engineering, Faculty of Engineering, Universitas Riau, Pekanbaru, Indonesia
[2] Department of Electrical Engineering, Faculty of Engineering, Ming Chi University of Technology, Taiwan
Email: yusnita.rahayu@lecturer.unri.ac.id (Y.R.), dimas.rama3721@student.unri.ac.id (D.R.A.P.), kuchiahao@mail.mcut.edu.tw (C.H.K.)

Manuscript received July 24, 2024; revised October 17, 2024; accepted November 20, 2024
*Corresponding author

***Abstract*—This research investigates a compact Asymmetric Coplanar Strip (ACS) fed monopole antenna that generates three frequency bands in wireless communication applications. The antenna design combines the ACS-fed technique with C-shaped, inverted L and U-shaped radiating strip branches to downsize the antenna size and generate multi-band radiation. The antenna is implemented on an inexpensive FR-4 substrate measuring 20×9×1.6 mm³. A systematic parametric assessment that includes variations in the length and width of the radiating strip has been carefully carried out, identifying three optimal frequency operational modes for the proposed antenna using an EM simulator Ansoft HFSS. The impedance bandwidths of the lower, middle, and higher frequency modes are 320 MHz (2.31-2.63 GHz), 470 MHz (3.3-3.77 GHz), and 2820 MHz (5.12-7.94 GHz), respectively. At 2.5 GHz, 3.55 GHz, and 5.45 GHz resonant frequencies, the measured antenna gain parameters are 5.67 dBi, 5.21 dBi, and 4.56 dBi. Due to its compact form factor and stable characteristics, the proposed antenna design emerges as a promising solution for internal antenna implementation in the Internet of Things (IoT) devices, especially in the context of wireless local area networks (WLAN), worldwide interoperability for microwave access (WiMAX), 5G sub-6GHz, and vehicle-to-everything (V2X) applications.**

***Index Terms*—Triple-band antenna, ACS-fed, IoT device, wireless network, V2X**

I. Introduction

The fast advancement of wireless communication systems has increased the demand for fast, reliable, and pervasive connectivity, especially for IoT devices. It is reported that before 2020, 25 billion devices were connected with 50 billion permanent connections and more than 200 billion intermittent connections, while Strategy Analytics estimates that there will be 38 billion connections by the end of 2025 and 50 billion by 2030 [1]. IoT devices have the ability to connect various devices through internet networks that enable real-time data collection, exchange, automation, decision-making, and analysis [2]. Therefore, IoT devices can improve efficiency, convenience, and innovation, playing a crucial role in various fields such as healthcare, transportation, smart cities, agriculture, and manufacturing [3]. The efficiency of IoT devices is highly dependent on stable and widespread wireless connectivity. To fulfill this need, an internal antenna that can operate across multiple frequencies, such as WLAN, WiMAX, 5G, and V2X, on portable devices is required. Therefore, there is a need for small-sized antennas that can be easily integrated into IoT devices.

Several factors affect the size of an antenna, one of which is the selection of the antenna feeding methods. Three commonly used and highly regarded feeding methods in the research community are microstrip, coplanar waveguide (CPW), and ACS. These methods are favored due to their cost-effectiveness, straightforward design, broad impedance bandwidth, and omnidirectional radiation patterns [4]. Single-sided printing in CPW [5, 6] and ACS [7, 8] is relatively low-cost compared to microstrip feeding techniques. ACS feeding techniques can significantly reduce the size compared to microstrip or CPW feeding methods [9]. Importantly, this reduction in size does not compromise the antenna's performance characteristics.

Many studies have shown that antennas designed using the ACS-fed technique are capable of achieving good multiband performance. ACS-fed antennas are effective in supporting various network operations used by modern wireless communication standards, such as WLAN and WiMAX [10–14]. In addition, this technology also supports applications in 5G sub-6GHz networks with optimized performance [15–18]. Furthermore, ACS-fed antennas are able to meet the needs of V2X or vehicle-to-vehicle (V2V) [19–21].

In [22], integrating defected structures and ACS feeding, with a Circular Ring Resonator (CRR) in the ground plane and an inverted T-shaped slot on the radiation strip, resulted in a smaller triple-band antenna that reduces interference, suitable for WLAN/WiMAX operations. Increasing the fractal order of the Hilbert Curve Fractal Antenna (HCFA) coupled with ACS-fed can reduce the antenna size and obtain high performance in multiband applications [23]. A swastika-shaped monopole antenna with ACS feeding is designed for tri-band WLAN and

doi: 10.18178/ijeetc.14.1.43-50

WiMAX applications, consisting of mirrored C-shaped strips, L-shaped strips, and meandering strips with a partial ground plane [24]. The antenna adopts an inverted L-shape and a separate Rectangular Split Ring Resonator (RSRR) structure combined with an ACS feedline to reduce the antenna size and generate three resonant frequencies for multiband applications [25]. To achieve the desired dual-band frequencies for Long-Term Evolution (LTE) and mid-band 5G, a meandering line radiation structure and uniplanar design with ACS feed are used, significantly reducing the antenna size [26]. The monopole antenna was successfully downsized and produced four operating bands after combining a Split Ring Resonator (SRR), an inverted U-stub, and a Complimentary Split Ring Resonator (CSRR) on the ground plane [27]. An electrically small ACS-fed antenna for WiMAX and WLAN applications uses a metamaterial-inspired open SRR as the radiator, achieving four operating bands [28]. A compact dual-band antenna inspired by a uniplanar metamaterial (MTM) has a circular Closed Ring Resonator (CRR) radiating element on the outside, Non-Bianisotropic Split Ring Resonator (NB-SRR) on the inside, and a meander strip line connected by an ACS fed to reduce size and improve impedance matching [29]. The designed antenna features an HCFA fed with an ACS and loaded with metamaterial RSRR, resulting in multiband radiation and a compact size [30]. However, the dimensions of some of these antenna designs make them less adaptable when integrated into IoT devices as internal antennas.

Therefore, in this article, we propose the use of a printed monopole antenna with compact-sized triple-band capability. This antenna can be embedded inside IoT devices to support WLAN, WiMAX, sub-6 GHz 5G, and V2X operations. Most researchers have designed the ACS-fed antenna for one of the WLAN/WiMAX/sub-6 GHz 5G or V2X/V2V applications, but not all. This compact configuration includes C-shaped, inverted L, and U-shaped radiating strip branches to generate three different resonant modes with higher peak gain. In real application scenarios, the suggested antenna not only upholds a compact physical profile but also achieves good characteristics.

II. Antenna Design

The overall structure of the proposed compact monopole antenna for IoT device systems can be observed in Fig. 1. The antenna has a small size of 9×20 mm², printed on an FR-4 substrate with a thickness of 1.6 mm, permittivity, and loss tangent of εr = 4.4 and tan δ = 0.02 respectively, as illustrated in Fig. 1 (a). For ease of integration and compactness, the antenna's transmission line is fed using a 50 Ω ACS feeding technique and a partial ground plane on the front side, both connected with an SMA connector as shown in Fig. 1 (b). Therefore, the fabrication of the proposed antenna is realized using a single-sided metallization process. Fig. 1 (c) shows the physical manifestation of the proposed antenna.

To assess the proposed antenna's performance, Fig. 2 presents four stages of the modified antenna design's evolution using an EM simulator, Ansoft HFSS. Each evolution stage aims to meet the specifications of various frequency bands, such as WLAN, WiMAX, sub-6GHz 5G, and V2X.

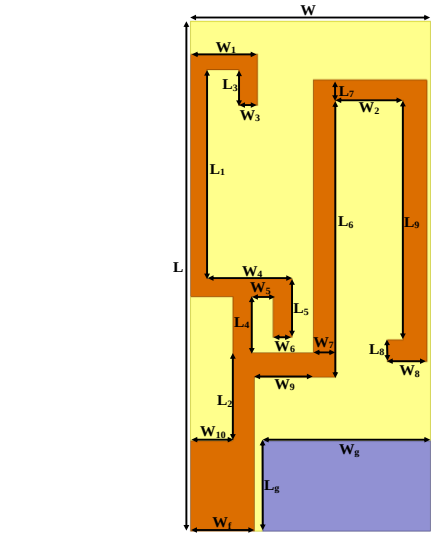

(a)

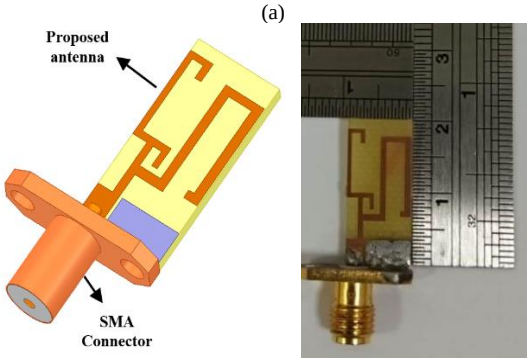

(b) (c)

Fig. 1. The proposed antenna geometry: (a) detailed dimensional design of the proposed antenna, (b) 3D visualization of the proposed antenna with SMA connector, (c) the physical manifestation of the antenna.

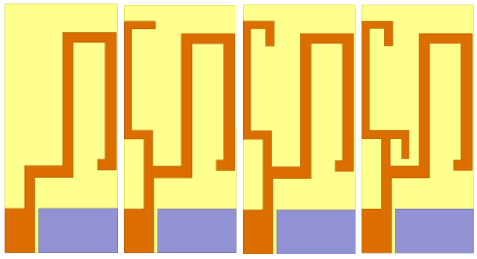

(a)

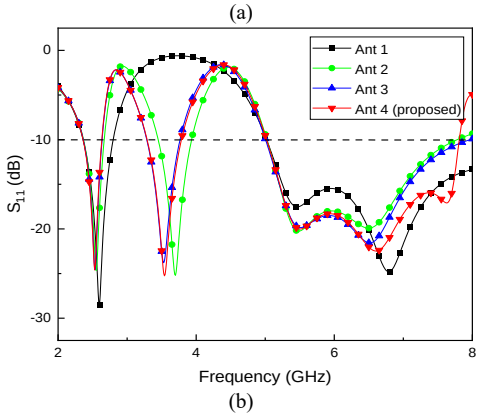

(b)

Fig. 2. (a) Evolution of antenna designs to the proposed model, (b) analysis of S11 responses from the evolution of the proposed antenna model.

TABLE I: OPTIMIZED VALUES OF THE PROPOSED ANTENNA

Parameter	Value (mm)	Parameter	Value (mm)
W	9	W_{10}	1.59
W_f	2.39	L	20
W_g	6.3	L_g	3.55
W_1	2.5	L_1	8.2
W_2	2.54	L_2	3.45
W_3	0.7	L_3	1.4
W_4	3.2	L_4	2.2
W_5	0.82	L_5	2.3
W_6	0.7	L_6	10.85
W_7	0.85	L_7	0.8
W_8	1.44	L_8	0.85
W_9	0.95	L_9	9.4

The first antenna (Ant 1) was designed as an inverted U-shaped meander with a long length designed to generate a frequency band at the lower resonant mode, which is dominated by the center frequency of 2.6 GHz. In addition, Ant 1 also stimulates a band in the higher resonant mode with an upper frequency of 5 GHz. Then, in the second stage (Ant 2), the antenna was adapted to target the middle band frequencies, with the modification of adding the length and configuration of the C-shaped radiating element effectively stimulating the 3.7 GHz middle band. Not only does Ant 2 stimulate the mid-band frequencies, but it also shifts the resonant frequency of the lower modes to 2.5 GHz. In the third stage (Ant 3), a rectangular strip is placed at the end of the C-shaped radiating element to successfully shift the middle band to the resonant frequency of 3.5 GHz. Finally, adding an inverted L-shaped strip as in stage 4 (Ant 4) can deepen the reflection coefficient at higher bands and thus form the proposed antenna. Through evolutionary stages and a series of careful evaluations, the optimal parameters of the proposed antenna are finally determined and attached in Table I.

Furthermore, the effective bandwidth of the antenna is also checked with the antenna impedance, as plotted in Fig. 3. By adjusting the antenna impedance including the real and imaginary parts (resistance and reactance) located in the desired frequency band, it can achieve a definition bandwidth of 10 dB, while the following conditions are satisfied simultaneously. In general, these conditions are that the resistance value is controlled in the range of 20 Ω to 75 Ω and the reactance value in the range of –25 Ω to 25 Ω. The Ant 1 structure achieves excellent matching at 2.6 GHz, (resistance and reactance are close to 50 Ω and 0 Ω, respectively), so the reflection coefficient of Ant 1 reaches as deep as 24 dB. Furthermore, by adding a C-shaped radiating element to form Ant 2, it effectively stimulates the 3.7 GHz middle band and shifts the lower frequency band to the 2.5 GHz resonance. Additionally, Ant 3 and Ant 4 offer good band matching at 3.5 GHz and deepen the reflection coefficient at higher bands, to fulfill the final antenna design.

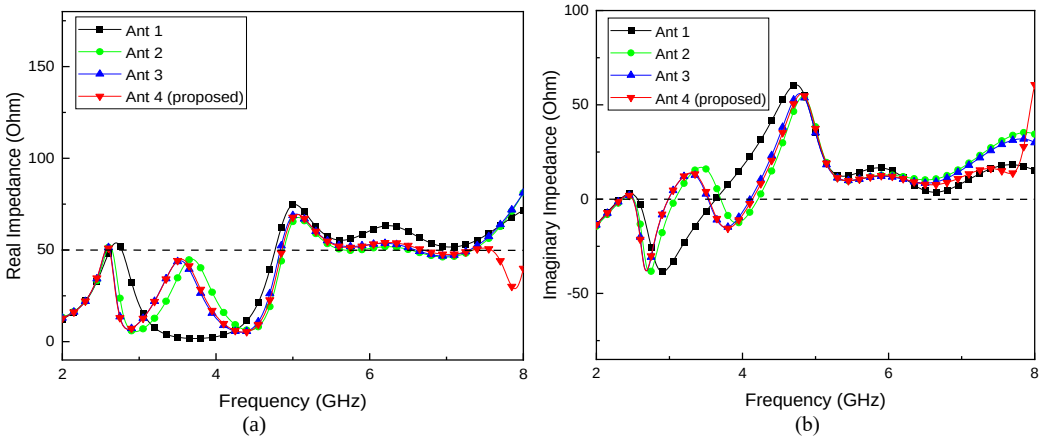

Fig. 3. Model impedance of the four proposed antenna stages. (a) real part and (b) imaginary part.

III. RESULTS AND DISCUSSIONS

A. S_{11} and VSWR Measurement

The antenna prototype was implemented by using a precise LPKF ProMat E33 circuit board etched machine and the measurement results were carefully measured by adopting a ShockLine MS46122A vector network analyzer. To compare the difference between the simulated and measured results, both results are plotted in Fig. 4. It can be observed that a slight deviation occurs in each band and this may come from the manufacturing process of the antenna and the connection between the SMA connector and the antenna. It can be found that the measured and simulated results are consistent according to the −10-dB impedance bandwidth, the measured reflection coefficient can cover 2.31 GHz to 2.63 GHz, 3.3 GHz to 3.77 GHz, and 5.12 GHz to 7.94 GHz.

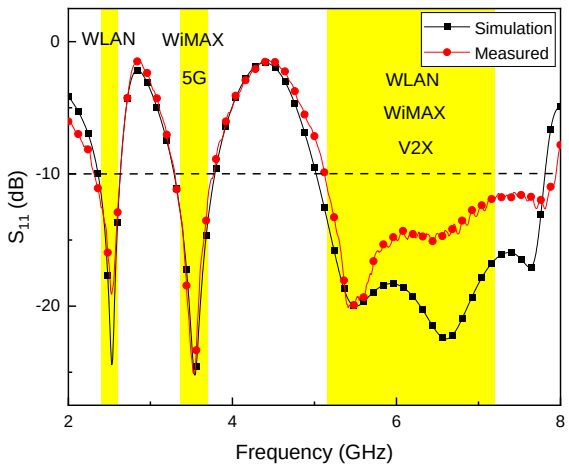

Fig. 4. Comparison of simulated and measured antenna S_{11} results.

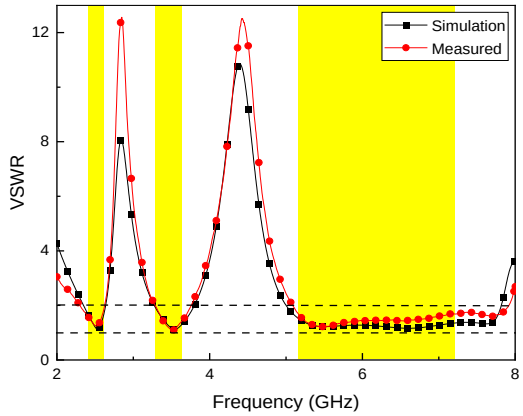

Fig. 5. Comparison of simulated and measured antenna VSWR results.

In addition, the VSWR measurement results, according to the general rule, can also be considered good; a value below 2:1 is considered good because it indicates that the majority of the energy emitted by the transmitter is successfully received by the antenna with little reflection, as shown in Fig. 5.

B. Current Distribution

The resonance mechanism of the monopole-type antenna is dominated by the guided quarter wavelength resonance [21], described as

$$\lambda = \frac{c}{4f\sqrt{\varepsilon_{\text{eff}}}} \tag{1}$$

$$\varepsilon_{\text{eff}} = \frac{\varepsilon_r + 1}{2} \tag{2}$$

where λ is the wavelength in free space, c represents the speed of light (3×10^8 m/s), f and ε_{eff} are the antenna working frequency and the effectiveness of some selected substrates. For further study of the resonant characteristics, simulation of the antenna current distribution using the Ansoft HFSS package will also be introduced in the next section.

The designed pattern is installed on the top of the system base plane; corresponding branch strips are added to drive the lower, medium, and higher bands of the proposed antenna. In accordance with the triple band resonance, the simulated current distributions at various resonant frequencies (2.53 GHz, 3.54 GHz, 5.51 GHz, and 6.62 GHz) will be executed as follows. For a clearer picture, the point-labeled map with detail marks is plotted in Fig. 6 (a), and the three simulated antenna current distributions at the previously mentioned frequencies are also plotted in Fig. 6 (b) to Fig. 6 (e), respectively. Fig. 6 (b) is the simulated current distribution when excited at 2.53 GHz. It is noted that the strong current density mainly flows along the right outer branch line (A-B-D-C-D line), whose length is estimated to be 30.2 mm and is close to a quarter of the wavelength of 2.53 GHz. In addition, the proposed antenna adopts a C-shaped strip in the left part to stimulate mid-band resonance. Fig. 6 (c) displays the maximum current density flow along the vertical branch lines (lines A-E-F), when the antenna is excited at 3.53 GHz. The length of the main current distribution is 19.24 mm, which is equivalent to a quarter of the 3.53 GHz wavelength. In addition, Fig. 6 (d) shows the most current flow along paths A-B and C-D, which gives a higher band resonance of 5.51 GHz, and 6 (e) shows 6.62 GHz (path A-B), respectively.

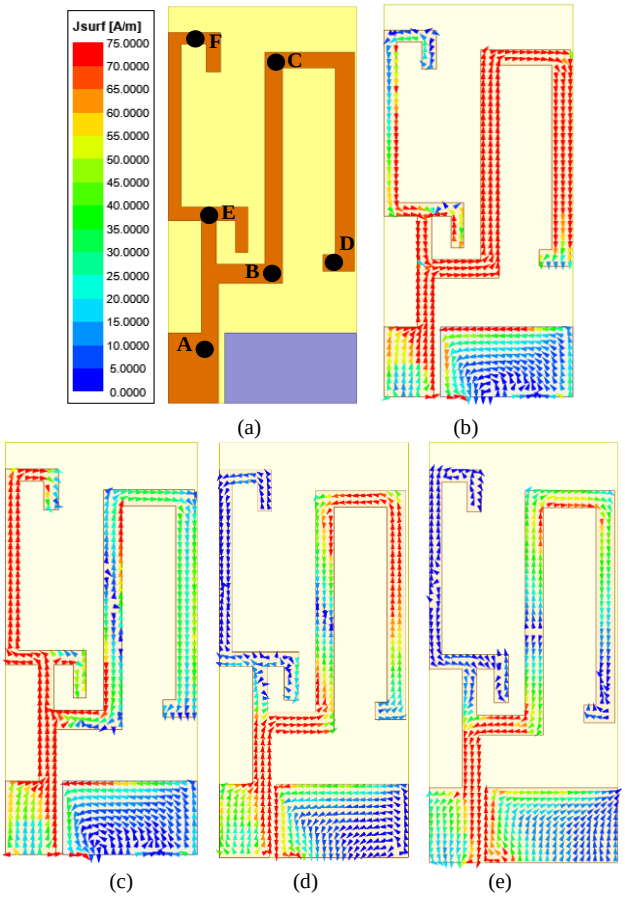

Fig. 6. Simulated results of antenna current distribution at (a) label-dot map, (b) 2.53 GHz, (c) 3.54 GHz, and (d) 5.51 GHz, (d) 6.62 GHz.

C. Parametric Study

To further evaluate the characteristics of the proposed antenna, three important parameters (W_1, W_7, L_7, L_9) are selected for parametric study in this section. Fig. 7 shows the reflection coefficient of the antenna design with different width variations of W_1 (2 mm, 2.5 mm, and 3 mm).

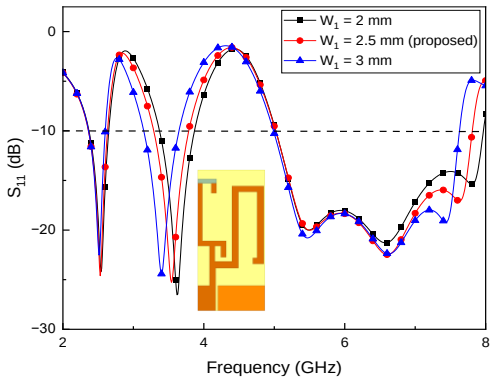

Fig. 7. Simulated results of antenna reflection coefficient with various values of W_1.

As mentioned earlier, the W_1 parameter is located in the C-shape strip section, which is the main path of mid-band

resonance. The wider the W_1 path, the intermediate frequency band will shift to a lower frequency. Meanwhile, the three results of varying the W_1 values for the lower band and the high band cover the proposed band range. Through careful calculation, the optimized W_1 value is finally selected to be 2.5 mm and can achieve the proposed mid-band to cover completely from 3.3 to 3.7 GHz.

Fig. 8 shows the effect of W_7 variation on the reflection coefficient results of the antenna design. W_7 is a significant factor that affects the lower and higher bands as W_7 is in the resonance path of both bands. Increasing the value of W_7 will shift the lower frequency band to higher frequency and the higher frequency band to lower frequency. Through careful simulation and evaluation, an optimized W_7 value of 0.85 mm was obtained. This value provides the best performance in balancing the shifting of the lower and higher frequency bands, achieving optimal reflection coefficient.

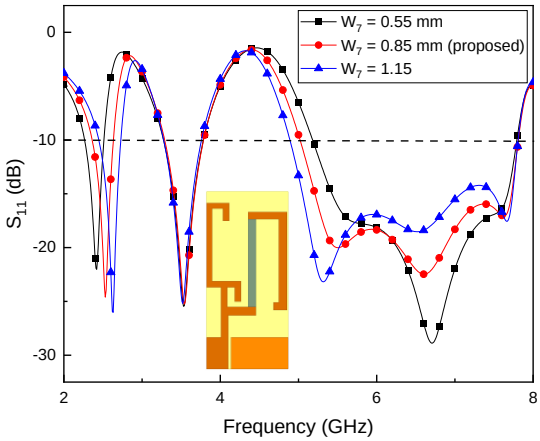

Fig. 8. Simulated results of antenna reflection coefficient with various values of W_7.

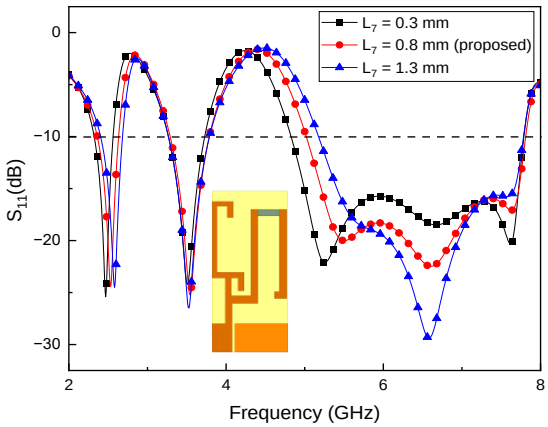

Fig. 9. Simulated results of antenna reflection coefficient with various values of L_7.

Furthermore, the L_7 parameter affects the reflection coefficient results of the entire antenna frequency band. As seen in Fig. 9, the larger the value of L_7, the overall frequency band will shift to a lower frequency. When L_7 = 0.3 mm, the lower frequency band does not cover the proposed band range. Meanwhile, when L_7= 1.3mm, the higher frequency band also does not cover the proposed band range. After careful evaluation, a value of L_7 = 0.8 mm was chosen because its reflection coefficient results cover the entire proposed frequency band.

In addition, the L_9 parameter can affect both the lower and higher bands as it is also the resonant path for both bands. The larger the L_9 value, both the lower and higher bands will shift to the lower frequency band. In Fig. 10, it can be seen that L_9 =9.4 mm is chosen because its reflection coefficient results cover all three proposed frequency band ranges.

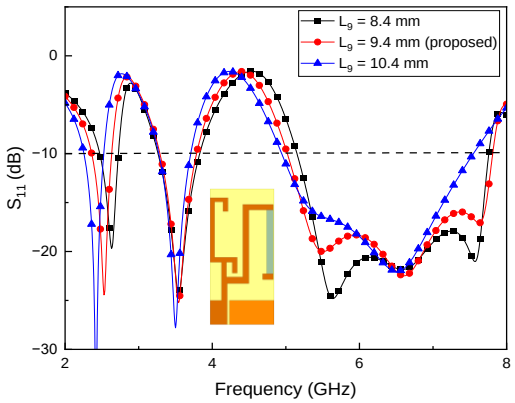

Fig. 10. Simulated results of antenna reflection coefficient with various values of L_9.

D. Radiation Pattern Measurement

In the context of antenna testing, aspects such as radiation pattern, gain, and efficiency are vital and must be tested in an anechoic chamber to prevent interference from surrounding electrical sources. The radiation performance of the designed antenna has been verified in an anechoic chamber. To demonstrate the antenna's performance at its intended working frequency, we selected three frequencies of 2.5 GHz, 3.55 GHz, and 5.45 GHz, each of which displays an optimal reflection coefficient to proceed. The radiation pattern of the tested antenna is shown in Fig. 11, where the YZ and XZ slices depict the E (Elevation) plane and the XY slice depicts the H (Azimuth) plane. From these measurements, it can be seen that the radiation patterns in the H and E planes indicate nearly omnidirectional and bidirectional characteristics across all targeted operational bandwidths.

In addition, the inherent peak gain and radiation efficiency of the antenna are also examined and verified inside the far-field anechoic chamber as mentioned earlier. All the experimental results, including peak gain and radiation efficiency, can be seen in Fig. 12. Meanwhile, the experimental values of peak gain range between the bands of 2.31 GHz to 2.63 GHz, 3.3 GHz to 3.77GHz, and 5.12 GHz to 6 GHz and vary between 2.4 dBi to 3.7 dBi, 3.6 dBi to 5.6 dBi and 5.7 GHz to 7.6 dBi respectively. In addition, the experimental efficiency from Fig. 9, the values show that the results range between 45% to 50%, 43% to 71%, and 52% to 90% across the three operating bandwidths. With a smaller size and simple structure, the proposed antenna has good performance, which includes not only sufficient impedance bandwidth and satisfactory efficiency but also omnidirectional and bidirectional radiation patterns in both horizontal and vertical planes. In addition, this antenna has a multiband operation that easily

includes WLAN, WiMAX, sub-6GHz 5G, and V2X bands. It can achieve various communication standard specifications and is a good candidate for IoT device antennas.

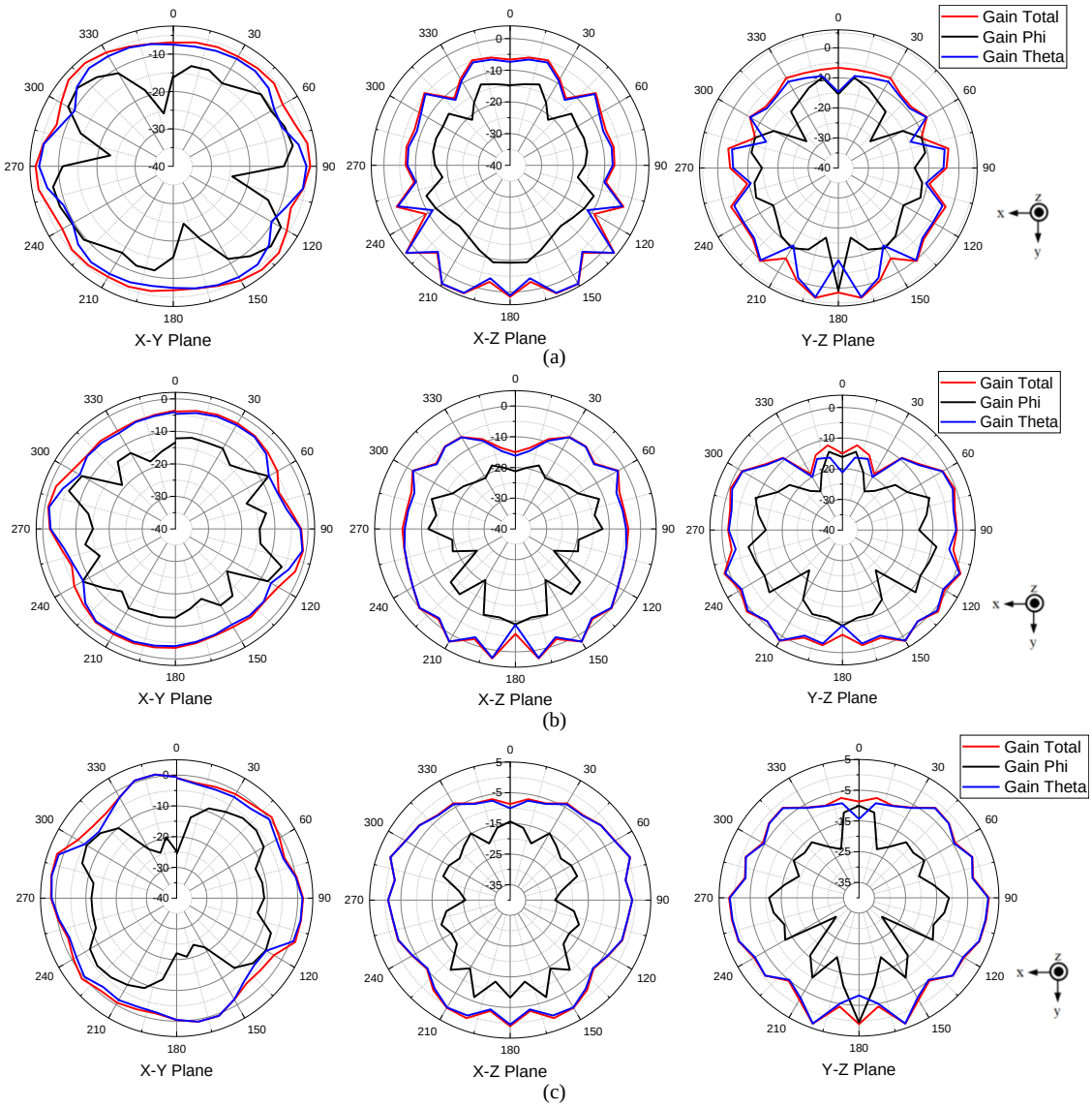

Fig. 11. Measured antenna radiation patterns results at (a) 2.5 GHz, (b) 3.55 GHz and (c) 5.45GHz.

TABLE II: PERFORMANCE COMPARISON OF THE PROPOSED WORK WITH OTHER ACS-FED ANTENNAS

Ref.	Resonance frequency (GHz)	Type of band	Bandwidth (MHz)	Peak gain (dBi)	Size (mm^2)
[22]	2.4/3.5/5.2	Triple-band	340/390/1110	3.3/4/7	$0.2\lambda_0 \times 0.096\lambda_0$
[23]	1.58/3.07/5.5	Triple-band	120/320/2360	0.27/1.33/2.27	$0.0948\lambda_0 \times 0.087\lambda_0$
[24]	2.4/3.5/5	Triple-band	200/540/900	1.8 (Avg)	$0.172\lambda_0 \times 0.112\lambda_0$
[25]	2.45/5.5/7.5	Triple-band	560/680/3000	1/3.1/3.7	$0.176\lambda_0 \times 0.096\lambda_0$
[26]	2.35/3.6	Dual-band	120/300	NA	$0.13\lambda_0 \times 0.083\lambda_0$
[27]	2.46/5.8/6.78/10.4	Quad-band	270/340/180/1160	1.3/2.43/2.61/3.15	$0.186\lambda_0 \times 0.11\lambda_0$
[28]	2.64/3.36/4.38/5.2	Quad-band	220/160/270/390	1.2/2.33/2.75/2.66	$0.136\lambda_0 \times 0.158\lambda_0$
[29]	3.2/4.85	Dual-band	230/1500	2.8 (Avg)	$0.253\lambda_0 \times 0.124\lambda_0$
[30]	1.4/4.4/5.3	Triple-band	330/570/340	0.37/1.37/1.68	$0.084\lambda_0 \times 0.077\lambda_0$
This work	2.5/3.55/5.45	Triple-band	320/470/2820	5.67/5.21/4.56	$0.167\lambda_0 \times 0.075\lambda_0$

Table II provides a comparison of the performance of the proposed antenna with other antennas using the ACS-fed technique. From this table, it can be seen that the antenna described in this study has the most compact size compared to other antennas, which is only 20×9 mm². Despite its smaller size, this antenna still exhibits optimal performance with effective triple-band operation capability, as reflected by its bandwidth and peak gain. This shows that the proposed antenna is not only smaller but also efficient in maintaining good performance quality across multiple frequency bands.

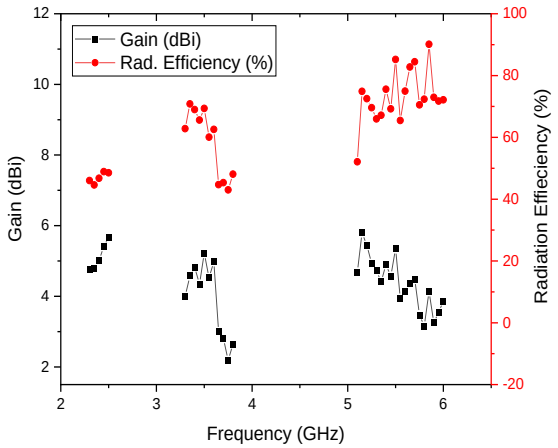

Fig. 12. Measured antenna peak gain and radiation efficiency results.

IV. Conclusion

A compact ACS-fed monopole antenna with three frequency band modes is investigated in this paper. ACS feedline connected with C-shaped, inverted L, and U-shaped radiating strip branches are printed on a 20×9×1.6 mm^3 FR-4 substrate. The measurement results of the fabricated antenna have good characteristics demonstrated through empirical measurements, focusing on parameters such as impedance bandwidth, gain, efficiency, and near-field pattern. The antenna operates in the frequency ranges of 2.31 GHz to 2.63 GHz, 3.3 GHz to 3.77 GHz, and 5.12 GHz to 7.94 GHz making it suitable for WLAN, WiMAX, sub-6GHz 5G, and V2X wireless applications. Antennas with compact size, and good performance are potentially good candidates for IoT devices.

Conflict of Interest

The authors declare no conflict of interest.

Author Contributions

Yusnita Rahayu and Chia Hao Ku formulated the basic idea for the antenna design, provided guidance and supervision throughout the research process and analysis, and offered invaluable suggestions for improving and refining the manuscript. With their contributions, Dimas Rama Adji Pangestu completed the research and writing this paper; all authors approved the final version.

References

[1] J. S. Yalli, M. H. Hasan, and A. Badawi, "Internet of things (IoT): origin, embedded technologies, smart applications and its growth in the last decade," *IEEE Access*, vol. 12, pp. 91357–91382, 2024.

[2] W. A. Awan, Q. Hussain, A. Abbas, Md. A. Sufian *et al.*, "Compact size frequency-agile antenna enabling multi-mode functionality for Internet of things applications," in *Proc. 18th Eur. Conf. Antennas Propagation (EUCAP)*, 2024. doi:10.23919/EuCAP60739.2024.10501644

[3] A. Khanna and S. Kaur, "Internet of things (IoT), applications and challenges: A comprehensive review," *Wireless Personal Communication*, vol. 114, no. 2, pp. 1687–1762, 2020.

[4] A. Kumar, P. V. Naidu, M. E. Atrash, V. Kumar, and M. A. "Independent hook loop antenna for WLAN applications," *IETE J. Res.*, vol. 70, no. 5, pp. 4523–4530, 2023.

[5] A. M. Mehta, S. B. Deosarkar, and A. B. Nandgaonkar, "Design and development of CPW-fed miniaturized MSA for improved gain, bandwidth and efficiency using PRS," *Prog. Electromagn. Res. C*, vol. 137, pp. 211–222, 2023. doi:10.2528/PIERC23071403

[6] M. S. Jameel, Y. S. Mezaal, and D. C. Atilla, "Miniaturized coplanar waveguide-fed UWB antenna for wireless applications," *Symmetry*, vol. 15, no. 3, p. 633, 2023.

[7] M. K. V. Subbareddy, D. D. Prasad, V. L. N. P. Ponnapalli *et al.*, "Asymmetric fed quad band monopole antenna for 5G and space applications," in *Proc. 2021 IEEE Int. Conf. Emerg. Trends Ind. 4.0*, 2021. doi:10.1109/ETI4.051663.2021.9619216

[8] M. Koohestani, N. Azadi-Tinat, and A. K. Skrivervik, "Compact slit-loaded ACS-fed monopole antenna for Bluetooth and UWB systems with WLAN band-stop capability," *IEEE Access*, vol. 11, pp. 7540–7550, 2023.

[9] J. Pathak and R. Labade, "Comparative analysis of microstrip feed, CPW feed & ACS feed UWB antenna," in *Proc. 2017 Int. Conf. Data Manag. Anal. Innov.*, 2017, pp. 285–289.

[10] K. A. Ansal, C. S. Ragamalika, C. Susan Rajan, and S. M. Baby, "A novel ACS fed antenna with comb-shaped radiating strip for triple band applications," *Mater. Today Proc.*, vol. 51, pp. 332–338, 2021. doi: 10.1016/j.matpr.2021.05.429

[11] A. Kumar, A. Jindal, A. Singh, R. Roy, O. P. Kumar, and T. Ali, "A closed modified V-shaped uniplanar triple band ACS fed antenna for wireless applications," *Bull. Electr. Eng. Informatics*, vol. 9, no. 4, pp. 1497–1505, 2020.

[12] S. N. Peerzade and S. Mudda, "A compact Asymmetric Coplanar Strip (ACS) antenna for WLAN and Wi-Fi applications," in *Proc. 2023 Int. Conf. Emerg. Smart Comput. Informatics*, 2023. doi: 10.1109/ESCI56872.2023.10099898

[13] P. V. Naidu, S. H. Akkapanthula, A. Kumar *et al.*, "ACS fed low profile goose shaped antenna for 5G wireless applications," in *Proc. 3rd Int. Conf. Range Technol.*, 2023. doi: 10.1109/ICORT56052.2023.10249119

[14] M. A. Abdalla and A. A. Ibrahim, "Open/short circuit terminations of efficient ACS-fed CRLH small antennas," *Analog Integr. Circuits Signal Process.*, vol. 102, no. 3, pp. 563–569, 2020.

[15] M. A. Reddy, A. R. Jency, S. Shabdita, and R. Pandeeswari, "A novel CSRR loaded compact ACS fed monopole antenna for sub-6 GHz 5G applications," *Prog. Electromagn. Res. Lett.*, vol. 106, pp. 89–95, Aug. 2022.

[16] K. Naveen, P. V. Naidu, V. N. Rao *et. al.*, "A small size triband dual l-shaped and pulse shaped compact size monopole antenna for 5G/wireless portable devices," *Mater. Today Proc.*, vol. 74, pp. 141–145, 2021. doi: 10.1016/j.matpr.2022.08.035

[17] S. L. Gunamony, G. J. Bala, S. M. G. Raj, and C. B. Pratap, "Asymmetric coplanar strip-fed electrically small reconfigurable 5G mid-band antenna," *Int. J. Commun. Syst.*, vol. 34, no. 15, pp. 1–11, 2021.

[18] U. Sharma, G. Srivastava, M. K. Khandelwal, and R. Roges, "Shorting pins-based triple band circularly polarized modified monopole compact dual-port MIMO antenna for sub-6 GHz wireless applications," *AEU - International Journal of Electronics and Commun.*, vol. 176, 2024. doi: 10.1016/j.aeue.2024.155162

[19] P. V. Naidu, M. B. Dhanekula, K. M. Almustafa *et. al.*, "Design and performance analysis of MAZE shaped quad port ACS fed tri-band MIMO antenna for V2V and multi-band applications," *AEU - International Journal of Electronics and Communications*, vol. 134, 2021. doi: 10.1016/j.aeue.2021.153676

[20] P. V. Naidu, D. Maheshbabu, A. Saiharanadh, A. Kumar, N. Vummadisetty, L. Sumanji, and Khalim A. Meerja, "A compact four-port high isolation hook shaped ACS fed mimo antenna for dual frequency band applications," *Prog. Electromagn. Res. C*, vol. 113, pp. 69–82, Apr. 2021.

[21] K. Sreelakshmi, "Compact ACS-fed frequency reconfigurable octa-band antenna for wireless portable systems," *Int. J. Numer. Model. Electron. Networks, Devices Fields*, vol. 37, no. 2, pp. 1–16, 2024.

[22] A. K. Abbas and S. Thangavelu, "Compact ACS-fed monopole antenna with CRR defect for triple band application," *AEU - International Journal of Electronics and Communications*, vol. 127, 2020. doi: 10.1016/j.aeue.2020.153487

[23] R. S. Daniel, "Asymmetric coplanar strip-fed with Hilbert curve fractal antenna for multiband operations," *Wirel. Pers. Commun.*, vol. 116, no. 1, pp. 791–803, 2021.

[24] P. V. Naidu, A. Kumar, R. R. Kumar *et. al.*, "Design, simulation and analysis of swastika shape uniplanar ACS fed antenna for multiple frequency band operation," in *Proc. 2020 IEEE Int. Women Eng. Conf. Electr. Comput. Eng.*, 2020, pp. 48–51.

[25] R. Rengasamy, V. Rajesh Kumar, and K. V. Phani Kumar, "An electrically small inverted L-shaped asymmetric coplanar strip-fed antenna with split-ring resonator for multiband applications," *Int. J. Commun. Syst.*, vol. 34, no. 17, pp. 1–17, 2021.
[26] S. L. Gunamony, J. B. Gnanadhas, and D. E. Lawrence, "Design and investigation of a miniaturized single-layer ACS-fed dual band antenna for LTE and 5G applications," *J. Electromagn. Eng. Sci.*, vol. 20, no. 3, pp. 213–220, 2020.
[27] P. N. Pillai and R. Pandeeswari, "Electrically small asymmetric coplanar strip-fed metamaterial-inspired antenna for WLAN and satellite-based applications," *Microw. Opt. Technol. Lett.*, vol. 65, no. 2, pp. 632–639, 2023.
[28] P. N. Pillai and R. Pandeeswari, "Asymmetric coplanar strip-fed electrically small metamaterial inspired antenna for quadband operation," *Prog. Electromagn. Res. Lett.*, vol. 107, no. September, pp. 59–66, 2022.
[29] P. N. Pillai and R. Pandeeswari, "A compact uniplanar ACS-fed metamaterial inspired dual band antenna for S-band and C-band applications," *Appl. Phys. A Mater. Sci. Process.*, vol. 128, no. 4, pp. 1–13, 2022.
[30] S. Rajapriya and R. S. Daniel, "Artificial neural network-based multiband μ-negative Hilbert curve fractal antenna using RSRR unit cell," *Telecommun. Syst.*, vol. 86, no. 1, pp. 189–200, 2024.

Yusnita Rahayu was born in Pekanbaru, Indonesia. She received a B.Eng degree in electrical engineering from the Department of Electrical Engineering, National Institute of Science and Technology Jakarta, in 1999. She received her M.Eng and Ph.D degrees from Universiti Teknologi Malaysia in 2004 and 2009, respectively. She is currently a senior lecturer in the Department of Electrical Engineering, at Universitas Riau. She is a senior member of IEEE. Her research interests include antenna and propagation, microwave and millimeter wave components, sensors, and wireless communication.

Dimas Rama Adji Pangestu is currently an undergraduate student in the Department of Electrical Engineering at Universitas Riau, Pekanbaru, Indonesia, since 2020. Additionally, he is pursuing a master's degree in the Department of Electrical Engineering at Ming Chi University of Technology (MCUT), New Taipei City, Taiwan, starting in 2024. He works as a research assistant in the Department of Electrical Engineering at MCUT, focusing on antenna design. His current research interests include antenna design, particularly for microwave, satellite, and millimeter-wave applications.

Chia-Hao Ku received his B.S and M.S degrees in electrical engineering from National Taiwan University of Science and Technology (NTUST) of Taipei, Taiwan in 1994 and 1996 respectively, and also received Ph. D. degree from NTUST in 2006. He joined in electrical engineering in Ming Chi University of Technology, New Taipei, Taiwan as an associated professor in 2008 and worked as a professor in 2016. Currently, his research interest lies in the area of electromagnetics and light wave, and includes experimental, simulation, and theoretical studies in various applications of microwave, millimeter wave, THz and nano antennas technology.